

AD-A033 597

RHODE ISLAND UNIV KINGSTON DEPT OF OCEAN ENGINEERING
OPTIMIZATION OF THE ELECTROCHEMICAL HYDROGEN PERMEATION TECHNIQ--ETC(U)
OCT 76 R HEIDERSBACH, J JONES

F/6 11/6

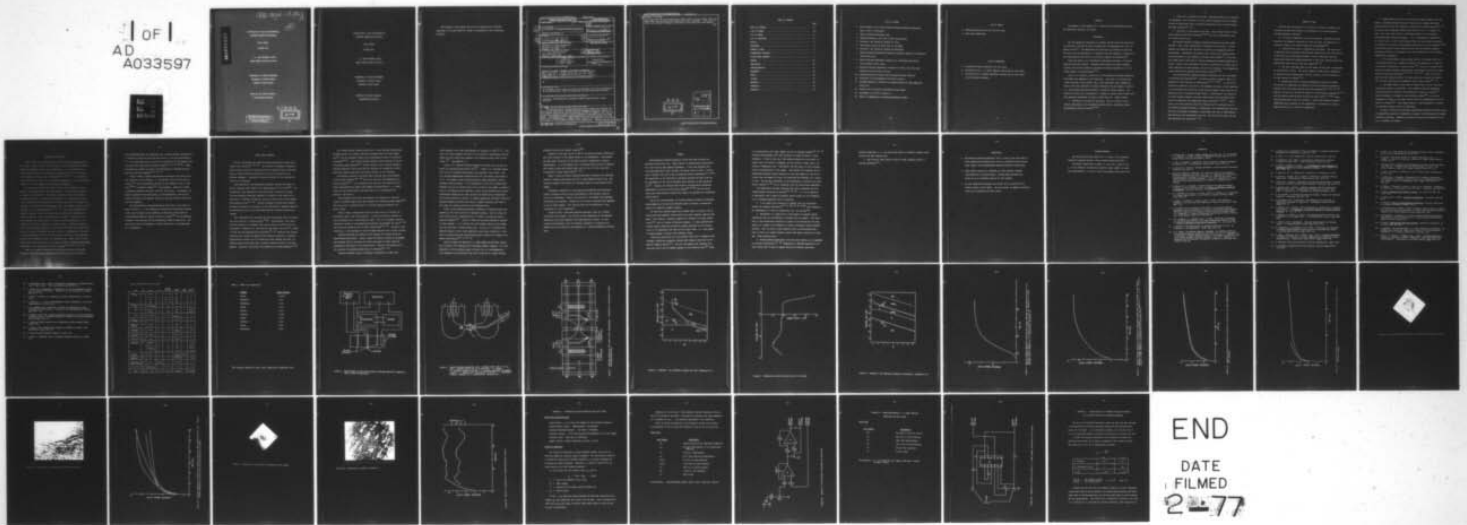
DAA629-76-G-0070

UNCLASSIFIED

ARO-13564.1-R-MS

NL

1 of 1
AD
A033597



020-13564. 1-R-025
✓
F.G.

(T2)

ADA033597

OPTIMIZATION OF THE ELECTROCHEMICAL
HYDROGEN PERMEATION TECHNIQUE

FINAL REPORT

OCTOBER 1976

U. S. ARMY RESEARCH OFFICE
GRANT NUMBER DAAG29-76-G-0070

DEPARTMENT OF OCEAN ENGINEERING
UNIVERSITY OF RHODE ISLAND
KINGSTON, RHODE ISLAND

APPROVED FOR PUBLIC RELEASE:
DISTRIBUTION UNLIMITED

DISTRIBUTION STATEMENT A
Approved for public release;
Distribution Unlimited

DDC
RECEIVED
DEC 16 1976
F

OPTIMIZATION OF THE ELECTROCHEMICAL
HYDROGEN PERMEATION TECHNIQUE

FINAL REPORT

OCTOBER 1976

U. S. ARMY RESEARCH OFFICE
GRANT NUMBER DAAG29-76-G-0070

DEPARTMENT OF OCEAN ENGINEERING
UNIVERSITY OF RHODE ISLAND
KINGSTON, RHODE ISLAND

APPROVED FOR PUBLIC RELEASE:

DISTRIBUTION UNLIMITED

The findings in this report are not to be construed as an official Department of the Army position, unless so designated by other authorized documents.

REPORT DOCUMENTATION PAGE		READ INSTRUCTIONS BEFORE COMPLETING FORM
1. REPORT NUMBER	2. GOVT ACCESSION NO.	3. RECIPIENT'S CATALOG NUMBER
4. TITLE (and Subtitle) OPTIMIZATION OF THE ELECTROCHEMICAL HYDROGEN PERMEATION TECHNIQUE.		7. TYPE OF REPORT & PERIOD COVERED Final rept.
7. AUTHOR(s) R. Heidersbach J. Jones		8. CONTRACT OR GRANT NUMBER(s) DAAG 29-76-G-0070 NEW
9. PERFORMING ORGANIZATION NAME AND ADDRESS Department of Ocean Engineering University of Rhode Island Kingston, RI 02881		10. PROGRAM ELEMENT, PROJECT, TASK AREA & WORK UNIT NUMBERS
11. CONTROLLING OFFICE NAME AND ADDRESS U. S. Army Research Office Post Office Box 12211 Research Triangle Park, NC 27709		12. REPORT DATE Oct 76
14. MONITORING AGENCY NAME & ADDRESS (if different from Controlling Office) 1251p.		13. NUMBER OF PAGES
		15. SECURITY CLASS. (of this report) Unclassified
		15a. DECLASSIFICATION/DOWNGRADING SCHEDULE NA
16. DISTRIBUTION STATEMENT (of this Report) Approved for Public Release; Distribution Unlimited 18) ARD 19) 13564.1-R-MS		
17. DISTRIBUTION STATEMENT (of the abstract entered in Block 20, if different from Report) NA		
18. SUPPLEMENTARY NOTES The findings in this report are not to be construed as an official Department of the Army position, unless so designated by other authorized documents.		
19. KEY WORDS (Continue on reverse side if necessary and identify by block number) Corrosion, electrochemistry, hydrogen, hydrogen embrittlement, metals, diffusion		
20. ABSTRACT (Continue on reverse side if necessary and identify by block number) An electrochemical hydrogen permeation cell incorporating improved geometrical and other design features has been developed and tested. Results on iron samples indicate the need for palladium coating of hydrogen entry and exit surfaces if internal transport rates of hydrogen in the metal are to be determined. Electrodeposition and vapor deposition of palladium coatings have been shown to be unsatisfactory. Samples vacuum coated by ion deposition in an argon plasma at reduced pressure proved to be satisfactory. Results obtained in		

ABSTRACT (Continued)

this study indicate that substantially longer times to obtain steady states are needed than have previously been reported by some researchers. This would indicate that hydrogen transport rates would be lower than have been reported.

DDC
RECEIVED
DEC 16 1976
RECEIVED
F

ACCESSION for	
NTIS	White Section <input checked="" type="checkbox"/>
DDC	Buff Section <input type="checkbox"/>
UNANNOUNCED	<input type="checkbox"/>
JUSTIFICATION.....	
BY.....	
DISTRIBUTION/AVAILABILITY CODES	
Dist.	AVAIL. and/or SPECIAL
A	

TABLE OF CONTENTS

	PAGE
TABLE OF CONTENTS	ii
LIST OF FIGURES	iii
LIST OF TABLES	iv
LIST OF APPENDIXES	iv
PURPOSE	1
BACKGROUND	1
SUMMARY OF NEED	3
EXPERIMENTAL PROCEDURE	5
COATED ENTRY SURFACES	7
SUMMARY	11
CONCLUSIONS	14
ACKNOWLEDGEMENTS	15
REFERENCES	16
TABLES	20
FIGURES	22
APPENDIX A	38
APPENDIX B	41
APPENDIX C	43

LIST OF FIGURES

1. Block diagram of the electrochemical hydrogen permeation apparatus used in this investigation.
2. Typical hydrogen permeation cell.
3. Hydrogen permeation cell used in this investigation.
4. Potential - pH (Pourbaix) diagram for iron.
5. Polarization curve for Armco iron in 0.2N NaOH.
6. Potential - pH (Pourbaix) diagram for palladium.
7. Typical hydrogen permeation transient previously reported for palladium-coated Armco iron.
8. Typical hydrogen permeation transient for palladium-coated Armco iron obtained in this study.
9. Replicate hydrogen permeation transients for Armco iron with vapor deposited entry and exit surfaces.
10. Debonded palladium coating after prolonged hydrogen charging.
11. Blistering of electrodeposited palladium coating.
12. Hydrogen permeation transients for plasma-coated and vapor-deposited Armco iron.
13. Tarnish film on surface of palladium coated sample.
14. Micrograph of surface in Figure 13.
15. Effect of temperature on measured permeation current.

LIST OF TABLES

1. Hydrogen permeation data for iron and steel.
2. Armco iron composition.

LIST OF APPENDIXES

- A. Potentiostat design fabricated for this study.
- B. Regulated-current D. C. power supplies fabricated for this study.
- C. Calculations as to whether palladium coatings will be rate limiting for hydrogen transport.

PURPOSE

The purpose of this research was to optimize the electrochemical hydrogen permeation technique for metals.

BACKGROUND

The low temperature permeation of hydrogen through steel and other materials has been a subject of broad interest since the phenomenon was first reported in 1863⁽¹⁾. The phenomenon has been known and studied for more than 100 years, but the mechanism(s) of hydrogen entry and transport in metals remain controversial and subject to continuing research and discussion⁽²⁾.

While the subject is of considerable theoretical interest, it also has important practical aspects. Hydrogen embrittlement and stress corrosion cracking are serious engineering problems, and hydrogen permeation is an important aspect of these phenomena⁽³⁻⁹⁾.

Table 1 is a summary of some data on low-temperature hydrogen permeation rates which have appeared in the literature. From this it is obvious that a wide variation in data exists, and a given researcher cannot compare his results with those obtained in another laboratory with any degree of certainty. This problem has been discussed at length by several authors. The variation in data can be attributed to a number of causes, some of which have been generally recognized, and some of which have not. These include:

1. Variations in calculation technique. This is a matter of continuing controversy and no generally-accepted means of calculating hydrogen permeation rates now exists⁽¹²⁻¹³⁾.

2. Variations in hydrogen flux level. Hydrogen permeation is concentration dependent, and differences in inlet surface hydrogen flux can be demonstrated to drastically alter the hydrogen permeation rate in ferrous alloys and other materials^(14, 15).

3. Variation in inlet-surface reactions. Many authors resort to elaborate surface preparation procedures,⁽¹⁶⁻¹⁸⁾ but this, unfortunately, has not always been the case.

Two general methods of measuring hydrogen permeation have been widely reported. Both involve introduction of hydrogen into one side of a metal membrane and measuring the rate which it arrives at the opposite side of the membrane. Introduction of hydrogen into a metal from a gaseous phase has the advantage of easy control of relative inlet fluxes⁽¹⁷⁾, and it has been widely used in the study of elevated temperature hydrogen permeation in metals. However, this technique is limited to relatively low fluxes, and it cannot duplicate the high hydrogen flux levels of interest in low temperature stress corrosion and hydrogen embrittlement studies⁽¹⁹⁻²⁰⁾.

The electrochemical hydrogen permeation technique was first introduced by Devanathan and Stachurski⁽²¹⁾ and later refined by Bockris, Nanis, and coworkers at the University of Pennsylvania^(14, 16, 22-26). It has the advantages of simplicity, low cost of the equipment involved, and the possibility for measuring the effects of widely varying hydrogen inlet fluxes on the permeation rates of hydrogen through metals. Unfortunately, the method has not been uniformly applied, and many organizations have encountered difficulties in employing this supposedly simple technique^(13, 27-29). Variations in the data reported using this technique can be ascribed to all of the reasons discussed previously. Nonetheless, this technique has great promise and, with proper development, could produce the type of reproducible data which has been unavailable up to now. The need for such data has been well documented and discussed^(3, 11).

SUMMARY OF NEED

From the above discussions on limitations of present techniques, the following features would appear to be desirable for an electrochemical hydrogen permeation technique:

1. It should be applicable to any alloy system. Although the above discussion is primarily concerned with iron and steel, its application to aluminum, titanium, and uranium alloys has been proposed⁽¹⁶⁾.

2. Surface effects must be minimized or eliminated. The need exists to separate surface reactions (polarization, passivation) from bulk effects so that they can be separately analyzed. This is especially true for those metals where the hydrogen permeation is very slow, necessitating long experimental times even for very thin samples^(30, 31).

3. The same techniques used for bulk sample studies must be applicable to surface-entry studies. The need to compare, unequivocally, permeation of hydrogen through samples where the only variable is the introduction of an inlet surface is obvious⁽³⁻⁴⁾.

4. Unequivocal means of measuring temperature effects are needed. The effects of temperature on diffusivity have been studied by several researchers and "activation energies" have been reported^(19, 23-24, 26, 32). However, the fact that diffusivity seems to be concentration dependent^(14, 22) and that surface-entry blocking effects have been noted^(30, 32-34) leaves these determinations subject to question. None of the reported studies on temperature have accounted for the possibility of alterations in surface entry efficiency as a function of temperature.

5. Sample preparation must not introduce extraneous hydrogen into the sample. Increased hydrogen fluxes have been noted in samples which have been chemically etched when compared to mechanically abraded surfaces^(19, 30). This may be due to improved surface entry kinetics (i.e., a "cleaner" surface), but it may also be due to unintended alteration of the sample by electrochemically generated hydrogen. It is a thermodynamic impossibility to dissolve iron, or most other metals, without the simultaneous liberation of hydrogen in the acids or other aqueous media which have been reported⁽³⁵⁻³⁷⁾. Thus chemical etching raises questions about how much hydrogen trapping, microcrack initiation or extension, etc. has occurred prior to the intended experimental measurement.

6. The electrochemical cell geometry must be in accordance with best electrochemical practice. Adequate agitation, the elimination of traps for gas bubbles, minimization of crevice effects⁽³⁴⁾, the use of buffered inlet solutions whenever possible, and provision for mechanical abrasion and temperature control seem desirable^(17, 19, 30, 32-33, 38). None of the cells that have been reported meet all of these objectives, although the modular cell in use at the Naval Air Development Center comes closest^(16, 33).

7. The sample shape (a thin wafer or prism) used by all of the above-cited authors should be maintained. This geometry minimizes extraneous diffusion paths and simplifies the mathematical analysis of results⁽³⁹⁾. Greene recommends a cylindrical electrochemical sample⁽⁴⁰⁾, but many researchers have found a flat sample better insofar as reproducibility of surfaces is concerned⁽⁴¹⁾. This sample geometry is also preferable if studies of anisotropic materials are to be undertaken.

In order to optimize the desirable experimental parameters outlined above, an experimental program was undertaken to improve the electrochemical hydrogen permeation technique. Emphasis was placed on entry surface preparation and on cell geometry and design.

EXPERIMENTAL PROCEDURE

Table 2 shows the chemical analyses of the Armco iron samples used in this study. Figure 1 shows a block diagram of the electrochemical hydrogen permeation apparatus used in this investigation. It is essentially the same as first reported by Devanathan and Stachurski⁽²¹⁾, and it has been used elsewhere by a number of investigators^(19, 26-30, 34). The potentiostat fabricated for this study is described in Appendix A, and the regulated-current D. C. power supplies are described in Appendix B.

One side of the sample (the right, or exit, side in Figure 1) is exposed to an aqueous solution and maintained at a constant anodic potential by means of a potentiostat. The current necessary to hold this sample at the preset potential is allowed to equilibrate to a minimum current value. Once a steady state background level is reached (less than 1 microamp/cm²), hydrogen is introduced into the opposite side of the sample by means of electrolysis or by gas phase charging^(17, 19, 21). The atomic hydrogen which passes through the sample and reaches the exit surface is immediately oxidized to hydrogen ions by the potentiostatic circuit. The change in current necessary to maintain the exit surface at the preset potential is a measure of the flow of hydrogen to the exit surface. Immediate oxidation of all atomic hydrogen reaching the exit surface maintains the hydrogen content at (or near) the surface very close to zero. Measurements of the time to achieve measurable flux at the exit surface, the shape of the permeation buildup curve (measured current, or calculated flux, versus time), and the total steady state flux then can be related to sample thickness, experimental temperature, and a wide number of other variables^(19, 22-26, 30-32, 42).

There are a number of methods for calculating diffusivity and other parameters from the hydrogen permeation data obtained by this technique.

All are predicated upon the assumption that a steady hydrogen concentration is attained at both the inlet and exit surfaces. The exit concentration ($c = 0$) is relatively easy to attain, but variations in inlet hydrogen concentration have been noted by several authors^(19, 22, 38, 42-43). These variations may account for some of the differences in hydrogen mobility data which have been reported^(23, 30, 38).

Figure 2 shows a typical electrochemical permeation cell such as has been reported in the literature. It is modelled after the cell used at Cornell⁽¹⁹⁾ and is essentially the same as that reported in use at Ohio State⁽³⁰⁻³¹⁾, Watertown Arsenal⁽³⁹⁾, and elsewhere. There are a number of geometric problems associated with this cell design. As examples, gas bubble accumulation and inefficient, or nonreproducible, stirring may account for some of the apparent changes in hydrogen charging rates which have been reported.

The electrochemical hydrogen permeation cell used in this study is shown in Figure 3. It was designed to eliminate the undesirable features of the cells commonly in use elsewhere and optimize the principles of electrochemical apparatus design outlined by Greene,⁽⁴⁰⁾ and now generally accepted in the corrosion and electrochemical research communities. The ends of the cell are transparent to allow observation of the experiment as it progresses.

COATED ENTRY SURFACES

Several researchers have reported hydrogen permeation studies using coated inlet surfaces^(16, 19, 39). The coating is intended to produce an inert surface, minimizing corrosion effects on hydrogen entry, while supplying a readily permeable medium which is not rate controlling for hydrogen transport. Palladium is normally selected for this purpose because of its inertness.

Both electrolytic and electroless palladium coatings have been reported; typically these deposits are approximately 10^{-5} cm thick⁽¹⁹⁾. Unfortunately, these deposits are not always inert, and rust or tarnish film are sometimes observed, possibly at holidays in the coating or as the result of hydrogen "blistering" such as is often seen in high temperature hydrogen attack^(13, 39). Thicker palladium coatings might possibly decrease the presence of holidays, but the likelihood of hydrogen damage to the palladium layer or to the palladium-substrate interface would be increased.

Many researchers have abandoned the use of palladium coating on hydrogen inlet surfaces of ferrous alloys⁽⁴⁵⁻⁴⁶⁾. Unfortunately, this introduces the problem of a hydrogen inlet surface which is reactive with its environment. Examination of the potential -pH diagram for iron⁽⁵⁴⁾, Figure 4 (which has been experimentally confirmed)^(37, 41) indicates that surface reactions (ion buildup and passive film formation) resulting in hydrogen-entry blocking effects are to be expected in most aqueous solutions, especially during those times when a cathodic charging current is not being applied. Effects of this nature have reported on titanium samples^(16, 46).

Low current-density cathodic protection of inlet surfaces during hydrogen decay cycles (no intended measurable hydrogen inlet) has been attempted⁽²⁵⁾, but this approach ignores the mixed-potential nature of electrode interfaces⁽³⁵⁻³⁶⁾. Even during hydrogen charging, some corrosion of the inlet surfaces seems possible⁽³⁸⁾, and the sulfuric acid or sodium hydroxide solutions reported to have been used for charging can be expected to cause passivation during times when the charging circuit is not activated.

Electrolytic charging of uncoated entry surfaces using well-buffered acids has been reported,^(32, 38) and in one case this was supplemented by surface abrasion⁽³⁸⁾. It is interesting to note that the authors who have taken these precautions report lower apparent diffusivities (i. e., longer times to reach steady state) than those who have not compensated for passivity (see Table 1).

Total hydrogen flux levels are generally not reported, but they are lower for uncoated samples than those reported for palladium-coated samples⁽¹⁹⁾. This may be due to blocking effects of surface corrosion products or to other factors.

Figure 5 shows a polarization curve for Armco iron in 0.2N NaOH, the electrolyte used in this investigation. It shows that iron is reactive in this environment over a wide potential range. This is in agreement with the theoretical (Figure 5) and experimental potential -pH diagrams for iron^(37, 41) and with other studies on iron in basic electrolytes^(47, 48). Because of this reactivity, it was necessary to coat the sample surfaces with an inert coating.

Metallic palladium was chosen for this purpose for reasons which have been discussed previously. Figure 6 shows the Pourbaix diagram for palladium and indicates that no reaction with sodium hydroxide is likely under the experimental conditions of this investigation. However, the possibility of the formation of palladium hydride must be considered^(37, 45).

Reported transport rates for hydrogen in palladium are lower than

those reported by the same investigators for hydrogen in iron^(21, 25). However, the total transport rate will not be altered if the palladium surface layers are thin enough when compared to the substrate metal (iron in this study).⁽¹⁹⁾ (See Appendix C.)

Figure 7 is a typical hydrogen permeation transient that has been reported for palladium-coated Armco iron⁽¹⁹⁾. Figure 8 is a hydrogen permeation curve for palladium-coated Armco iron obtained in this study. The only intended experimental differences were the cell design (see Figures 2 and 3), the somewhat higher charging density, sample thickness, and the palladium coating process. It is interesting to note that a "steady-state" hydrogen flux was not reached after even 24 hours for the sample in Figure 8. Most of the hydrogen fluxes reported in Table 1 were obtained using similar experimental techniques and were normally calculated using "steady-state" flux levels obtained in minutes. No sample preparation techniques involving possible hydrogen evolution from water or aqueous solutions were used in this study for reasons which have been discussed above.

Figure 9 shows hydrogen permeation transients on replicate Armco iron samples for the first two hours of hydrogen charging. The two curves are quite similar and the reproducibility of fluxes is at least as good as reported elsewhere⁽¹⁹⁾. Figure 10 shows the long-term permeation behavior of these samples*. It is obvious that both samples require a much longer time than two hours to reach steady state. In fact, it is doubtful from examining Figure 10 that either permeation curve truly leveled off. This type of transient has been observed previously, although the reasons for it remain controversial^(13, 24, 39, 49).

Figure 11 shows the debonding of a vapor-deposited palladium coating from the Armco iron substrate after prolonged cathodic charging. It is not dissimilar to the blistering shown in Figure 12 on an electrodeposited

*One experiment was terminated after 22-1/2 hours due to a power failure.

palladium coating after similar exposure (39).

Failures of this type led to the use of an argon-ion plasma coating process after cleaning of the sample surface by ion bombardment. This process was done under subcontract by the Millis Research Corporation of Millis, Massachusetts. It is anticipated that a sputtered coating after ion bombardment cleaning would work equally well, and this has, in fact, been used successfully in other laboratories (16, 46).

Figure 13 shows successive hydrogen permeation transients for replicate samples of plasma-coated Armco iron and of vapor-deposited Armco iron. The long-term hydrogen flux levels are noticeably higher for the plasma-coated samples.

Microscopic examination of the plasma-coated samples after prolonged cathodic charging failed to locate any defects in the coating or any indications of debonding. However, the surface of the samples were sometimes discolored after exposure. Figures 14 and 15 show the tarnish which appeared on one of these samples. This tarnish could not be identified by X-ray diffraction or X-ray fluorescence.

Figure 16 shows a long-term hydrogen permeation curve for a plasma-coated Armco iron sample. The effects of room temperature on the measured permeation rate became apparent after approximately 24 hours. No true steady state permeation flux was obtained, although it is unclear as to whether or not it would have been observed in a constant-temperature environment.

SUMMARY

Electrochemical hydrogen permeation curves have been obtained for palladium-coated Armco iron. These indicate a substantially slower permeation rate than has been reported elsewhere. It has been suggested that the slower permeation rates (actually the longer times to reach a "steady-state" hydrogen flux) may be due to undesired surface degradation^(39, 45-46). The possibility of the formation of palladium hydrides has been cited for the abandonment of the use of palladium entry surfaces in some laboratories⁽⁴⁵⁾. However, the charging media used in electrochemical permeation experiments are reactive with ferrous alloys,^(32, 47-48) and this would cause worse entry-blocking effects than those to be expected on a palladium-coated surface.

The use of ion-bombardment for surface cleaning followed by subsequent plasma-deposition coating with palladium seems to produce a nonreactive surface for hydrogen transport studies.

The long-term hydrogen permeation buildups shown in Figures 9 and 12 would yield lower apparent diffusivities than those commonly reported elsewhere. This behavior, generally reported as "anomalous" by other laboratories⁽²⁴⁾, may be evidence of hydrogen trapping. It seems possible that similar results might have occurred on samples subjected to low charging rates if the experiments had been run for longer times, i.e., long enough to expose samples to similar total hydrogen fluxes.

Oriani has pointed out that low charging rates tend to emphasize bulk transport (diffusion) processes, whereas high charging rates tend to emphasize trapping effects⁽⁵⁰⁾. The fact that Bockris and coworkers have seen this effect only on samples exposed at high charging rates⁽²⁴⁾ leads

to the possibility that these "peaks" are due to hydrogen trapping^(12, 50, 59) occurring simultaneously with bulk migration by volume diffusion or other processes. If this be the case, then hydrogen permeation rates would increase until the effects of trapping, and the growth of traps, cause a reduction in permeation rate. Conceivably, the end result of such a process would be disintegration of the sample. Some authors have reported that reproducible hydrogen buildup transients on the same sample can only be obtained after the sample has first been saturated with hydrogen for a period of time. This has been attributed to the introduction or enlarging of traps during charging^(51, 52) and is consistent with the above-stated hypothesis.

This explanation has been discussed with other researchers who have reached similar tentative conclusions^(13, 39, 49). If it is accepted as an hypothesis, then a number of problems result insofar as the interpretation of hydrogen permeation data is concerned:

1. If no steady state condition is reached, then the calculation methods for hydrogen diffusivity^(12, 17, 19, 23, 26, 43-44) which depend on the measurement of a time to steady-state flux are invalid⁽⁴⁹⁾.

2. Degradation of a sample due to the presence of hydrogen begins immediately upon the introduction of hydrogen into the sample. This means that no true steady-state condition is likely to be obtained and the trap density of a sample can be expected to change continuously during hydrogen charging. This can occur at high charging rates in well-annealed pure iron, as well as in higher strength, higher trap density materials at somewhat lower charging rates.

3. Because hydrogen permeation rates have been reported to be dependent on hydrogen concentration^(14, 15) comparisons of hydrogen permeability between alloys must be made on samples which have undergone equivalent

charging conditions, i. e., the same total amount of hydrogen charging introduced at the same charging rate.

4. High charging rates should be used to study trapping effects on hydrogen permeation⁽⁵⁰⁾.

CONCLUSIONS

1. The optimized hydrogen permeation cell in Figure 3 has been shown to yield reproduceable hydrogen flux levels on palladium-coated ferrous alloy samples for electrochemical hydrogen permeation experiments.
2. Inert sample surfaces are necessary to study hydrogen transport characteristics of ferrous alloys. Plasma-coated palladium has proven to be an acceptable surface for this purpose.
3. No true steady-state hydrogen flux levels can be achieved for the steels studied in this report. For this reason, no apparent diffusivities can be calculated for these alloys.

ACKNOWLEDGEMENTS

This work was performed under the U. S. Army's Post Laboratory Cooperative Research Program, Contract Number DAAG29-76-G-0070.

The helpful cooperation of Messrs. M. Levy and T. Kelly of the U. S. Army Materials and Mechanics Research Center (AMMRC) is gratefully acknowledged. J. Kolts of Armco Steel supplied the Armco iron.

REFERENCES

1. H. Deville and L. Troost, *Comptes Rendes*, 57 (1863) 965, 977 (referenced in C. Kuehler, "A Study of Hydrogen Permeation Through Metals", Ph. D. Dissertation, Princeton University, 1974.)
2. J. Tien, A. Thompson, I. Bernstein, and R. Richards, "Hydrogen Transport by Dislocations," *Metallurgical Transactions A*, 7A (1976) 821.
3. J. Hirth and H. Johnson, "Hydrogen problems in energy-related technology", *Corrosion*, 32 (1976) 3.
4. Preliminary reports, memoranda, and technical notes of the Materials Research Conference, La Jolla, CA., Vol. II, "Degradation of Materials in Energy Related Systems in the Presence of Hydrogen, and Solar Energy Systems: Materials Problems," July 1974, Department of Materials and Metallurgical Engineering, University of Michigan (AD B 003586).
5. W. Reuter and C. Hartbower, "Stress-Corrosion and Hydrogen-Induced Cracking in D6aC Low-Alloy Steel", in Effect of Hydrogen on Behavior of Materials, TMS-AIME, New York, 1976, page 159.
6. P. A. Parrish, K. B. Das, C. M. Chen, and E. D. Verink, Jr., "Inhibition of Hydrogen Embrittlement of D6aC Steel in Aqueous Oxidizing Media", *ibid*, page 169.
7. J. Burke, A. Jickels, P. Maulic, and M. L. Mehta, "The Effect of Hydrogen on the Structure and Properties of Fe-Ni-Cr Austenite", *Ibid*, page 102.
8. W. Gerberich and D. Atteridge, "The Study of Dislocation Dynamics Associated with Ductile-Brittle Transition and Hydrogen Embrittlement Phenomena Observed in BCC Metals," Annual Technical Progress Report III, Department of Chemical Engineering and Materials Science, University of Minnesota, March 1975 (C00-2212-3).
9. B. C. Odegard, J. A. Brooks, and A. J. West, "The Effect of Hydrogen on the Mechanical Behavior of Nitrogen Strengthened Stainless Steel", in Effect of Hydrogen on Behavior of Materials, *loc. cit.*, page 116.
10. O. Gonzalez, "The Measurements of Hydrogen Permeation in Iron: An Analysis of the Experiments," *TAIME*, 245 (1969) 607.
11. B. F. Brown, "Preliminary reports, memoranda, and technical notes of the Materials Research Conference, La Jolla, CA, Vol II, "Degradation of Materials in Energy Related Systems in the Presence of Hydrogen, and Solar Energy Systems: Materials Problems," July 1974, Department of Materials and Metallurgical Engineering, University of Michigan (AD B 003586), Page 112.

12. G. Caskey and W. Pillinger, "Effect of Trapping on Hydrogen Permeation," *Metallurgical Transactions A*, 6A (1975) 467.
13. B. Wilde, U. S. Steel Corporation, private communication, July 1976.
14. T. Namboodhiri and L. Nanis, "Concentration Dependence of Hydrogen Diffusion in Armco Iron," *Acta Metallurgica*, 21 (1973) 663.
15. R. Oriani, "Hydrogen in Metals," in Proceedings of the Conference on Fundamental Aspects of Stress Corrosion Cracking, 1967, Columbus, OH NACE (1969) 32.
16. J. DeLuccia, Ph. D. Dissertation, University of Pennsylvania, 1976.
17. R. Miller, J. Hudson, and G. Ansell, "Permeation of Hydrogen Through Alpha Iron," *Metallurgical Transactions A*, 6A, (1975) 117.
18. C. Kim and A. Loginow, "Techniques for Investigating Hydrogen - Induced Cracking of Steels with High Yield Strength," *Corrosion*, 24 (1968) 313.
19. A. Kumnick and H. Johnson, "Hydrogen Transport Through Annealed and Deformed Armco Iron," *Metallurgical Transactions*, 5 (1974) 1199.
Also: A. Kumnick, Ph. D. Dissertation, Cornell University, 1972.
20. H. van Leeuwen, "A Quantitative Model of Hydrogen Induced Grain Boundary Cracking," *Corrosion*, 29 (1973) 197.
21. M. Devanathan and Z. Stachurski, "The Adsorption and Diffusion of Electrolytic Hydrogen in Palladium," *Proceedings, Royal Society*, 270A (1962) 90.
22. J. McBreen and M. Genshaw, "The Electrochemical Introduction of Hydrogen into Metals," in Proceedings, Fundamental Aspects of Stress Corrosion Cracking, loc. cit., p. 51.
23. J. Bockris, J. McBreen, L. Nanis, "The Hydrogen Evolution Kinetics and Hydrogen Entry into Alpha-Iron," *J. Electrochemical Society*, 112 (1965) 1025.
24. J. Bockris and P. Subramanyan, "Hydrogen Embrittlement and Hydrogen Traps," *J. Electrochemical Society*, 118 (1971) 1114.
25. M. Devanathan, Z. Stachurski, and W. Beck, "A Technique for Evaluation of Hydrogen Embrittlement Characteristics of Electroplating Baths," *J. Electrochemical Society*, 110 (1963) 886.
26. W. Beck, J. Bockris, and J. McBreen, and L. Nanis, "Hydrogen Permeation in Metals as a Function of Stress, Temperature, and Dissolved Oxygen Concentration," *Proceedings, Royal Society*, 290A (1966) 220.
27. R. McCright, Ohio State University, private communication, August 1975.
28. H. Pickering, Pennsylvania State University, private communication, July 1975.

29. M. Levy, U. S. Army Materials and Mechanics Research Center, Watertown, Mass., private communication, August 1975.
30. M. Fontana, "Corrosion Cracking of Metallic Materials, Part I - Summary," Ohio State University, August 1972, Report Number AFML-TR_72-102, Part I.
31. M. Fontana and R. Staehle, "Stress-Corrosion Cracking of Metallic Materials Part III - Hydrogen Entry and Embrittlement in Steel," Ohio State University, April 1975, Report AFML-TR-72-102, Part III.
32. J. Choi, "Diffusion of Hydrogen in Iron," Metallurgical Transactions, 1 (1970) 911.
33. P. Fisher and J. Jankowsky, "Determination of Hydrogen Generated by Paint Removers on Cadmium Plated Steel by the Electrochemical Permeation Method," Naval Air Development Center Report NADC-72045-VT, May 1972.
34. P. Hudson, E. Snavelly, J. Payne, L. Fiel, and N. Hackerman, "Absorption of Hydrogen by Cathodically Protected Steel," Corrosion, 24 (1968) 189.
35. H. Uhlig, Corrosion and Corrosion Control, John Wiley and Sons, New York, 1963.
36. M. Fontana and N. Greene, Corrosion Engineering, McGraw-Hill, New York 1967.
37. M. Pourbaix, Atlas of Electrochemical Equilibria, National Association of Corrosion Engineers, Houston, 1974.
38. R. McCright and R. Staehle, "Effect of arsenic upon the entry of hydrogen into mild steel as determined at constant electrochemical potential," Journal of the Electrochemical Society, 121 (1974) 609.
39. R. Heidersbach, "Permeation of hydrogen through electroslog-remelted 4340 steels," report submitted to U. S. Army Materials and Mechanics Research Center, August 1975.
40. N. Greene, Experimental Electrode Kinetics, Rennsalaer Polytechnic Institute, Troy, NY, 1965.
41. R. Cusamano, "The establishment of a three dimensional (potential - pH - composition) diagram for binary Fe-Cr alloys in 0.1 molar chloride solutions," M. S. Thesis, University of Florida, 1971.
42. W. Beck, J. Bockris, J. McBreen, and L. Nanis, "Hydrogen permeation in metals as a function of stress, temperature, and dissolved hydrogen concentration," Proceedings of the Royal Society, 290A (1966) 20.

43. T. Namboodhiri and L. Nanis, "Concentration dependence of hydrogen diffusion in Armco Iron," *Acta Metallurgica*, 21 (1973) 663.
44. L. Nanis and T. Namboodhiri, "Mathematics of the electrochemical extraction of hydrogen from iron," *Journal of the Electrochemical Society*, 119 (1972) 691.
45. L. Nanis, University of Pennsylvania, private communication, 8 August, 1975.
46. J. DeLuccia, U. S. Navy Air Development Center, Warminster, PA, private communication, 13 July, 1976.
47. C. M. Shepherd and S. Schuldiner, "Effect of Chloride Ion in Iron Corrosion in NaOH Solution," *Journal of the Electrochemical Society*, 119 (1972) 572.
48. S. Asakura and K. Nobe, "Electrodissolution Kinetics of Iron in Chloride Solutions, Part II: Alkaline Solution", *Journal of the Electrochemical Society*, 118 (1971) 19.
49. M. Louthan, duPont Savannah River Laboratory, private communication, August 1975.
50. R. Oriani, "The diffusion and trapping of hydrogen in steel", *Acta Metallurgica*, 18 (1970) 147.
51. S. Wach, *British Corrosion Journal*, 6 (1971) 114.
52. S. Wach, A. Miodownik, and J. Mackowiak, *Corrosion Science*, 6 (1966) 271.

TABLE 1. Hydrogen Permeation Data for Iron and Steel

SOURCE	YEAR	MATERIAL	TEMP(°C)	APPARENT DIFFUSIVITY ($\times 10^5$ cm ² /sec)	CHARGING MEDIUM	INLET COATING	CALCULATION METHOD
Nambodhiri and Nanis	1972	Armco Iron	22	2.14 - 3.48	NaOH	---	$t_{0.5}$
		Armco Iron	22	5.53 - 8.45	H ₂ SO ₄	---	$t_{0.5}$
		4340	22	0.667 - 1.140	NaOH	---	$t_{0.5}$
		4340	22	1.71 - 2.19	H ₂ SO ₄	---	$t_{0.5}$
Nambodhiri and Nanis	1970	Armco Iron 2% Cold Rolled	21	0.50	NaOH	---	$t_{0.5}$
Gileadi	1966	Armco Iron	27	2.0	NaOH	---	Unstated
		Fe-CR(10%)	27	0.002	NaOH	---	Unstated
Dillard	1972	Zone Refined Iron	24	7.0 - 7.8	H ₂ SO ₄ with AS ₂ O ₃	---	$t_{0.63}$
Bockris and Devanathan	1962	Armco Iron	25 ± 2	8.3	Various	---	$t_{0.63}$
Beck, Bockris, Genshaw, and Subramanian	1970	Armco Iron	27	5.0	NaOH	---	$t_{0.5}$
		Armco Iron	80	9.0	NaOH	---	$t_{0.5}$
Devanathan and Stachurski	1962	Armco Iron	24 ± 2	3.5 - 8.9	H ₂ SO ₄ and NaOH	---	$t_{0.63}$
Wach, Miodownik, Mackowiak	1966	High Purity Iron	25	2.5	Gas Phase	---	t_0
Fontana and Wang	1972	4340	25	.01 - .032	0.2N NaOH	---	$t_{0.5}$
Beck, Bockris, McBreen, Nanis	1965	Zone Refined Iron	25 ± 1	6.05	NaOH	---	Unstated
		Armco Iron	25 ± 1	6.02	NaOH	---	Unstated
		Armco Iron Single Crystal	25 ± 1	8.25	NaOH	---	Unstated
		4340	25 ± 1	.00251	NaOH	---	Unstated
Kumnick and Johnson	1974	Armco Iron	25	1.3	NaOH or Gas Phase	Some Pd	$t_{0.63}$
Berman, Beck and DeLuccia	1974	4340	25	.025	NaOH + NaCN	---	$t_{0.83}$
Beck, Bockris, McBreen, and Nanis	1966	4340	Unstated	0.11	NaOH + NaCN	---	$t_{0.5}$
Kim and Loginow	1968	3Ni - 1.5 Cr 0.5 Mo Steel	25	0.063 - 0.3	NaOH	---	$t_{0.63}$
Berman	1974	HY 130	25	0.01 - 0.04	Unstated	---	Unstated

TABLE 2: ARMCO Iron Composition *

<u>ELEMENT</u>	<u>WEIGHT PERCENT</u>
Carbon	0.00135
Manganese	0.045
Phosphorus	0.004
Sulfur	0.0025
Silicon	0.002
Nitrogen	0.0009
Copper	0.018
Chromium	0.006
Nickel	0.005
Molybdenum	0.005

* Heat analysis supplied by Armco Steel Corporation, Middletown, Ohio.

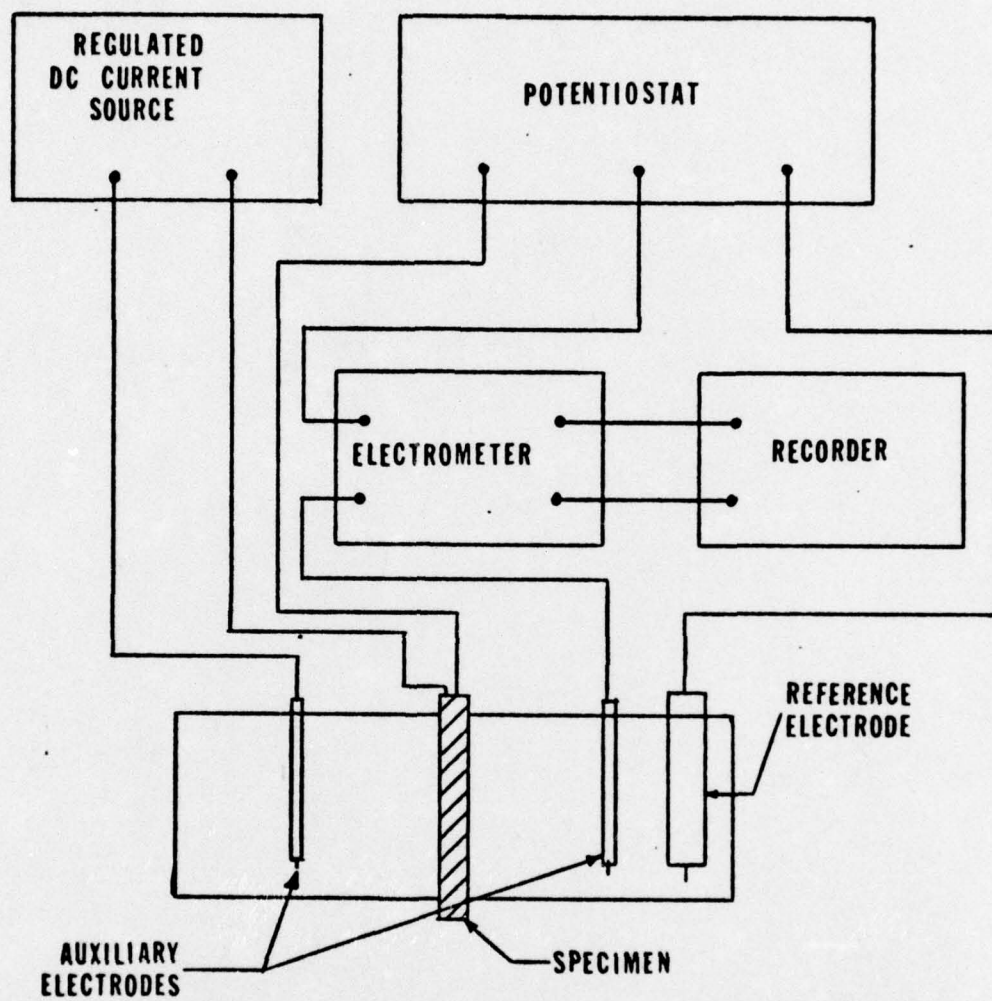


Figure 1: Block diagram of the electrochemical hydrogen permeation apparatus used in this investigation.

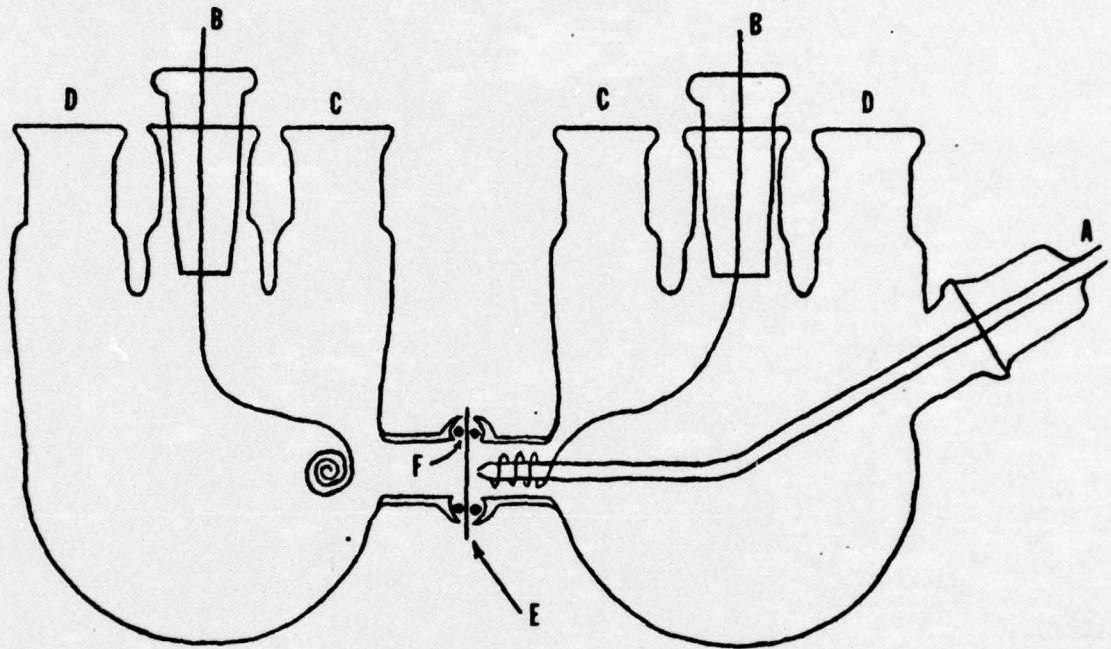


Figure 2: Typical hydrogen permeation cell. Hydrogen inlet cell is on the left. Hydrogen outlet cell is on the right. E = Sample, B = Platinum counter electrode, A = Reference electrode (saturated calomel), C = Sparging gas inlet/outlet (nitrogen), D = Thermometer (After A. Kmnick, Ph. D. dissertation, Reference 19.)

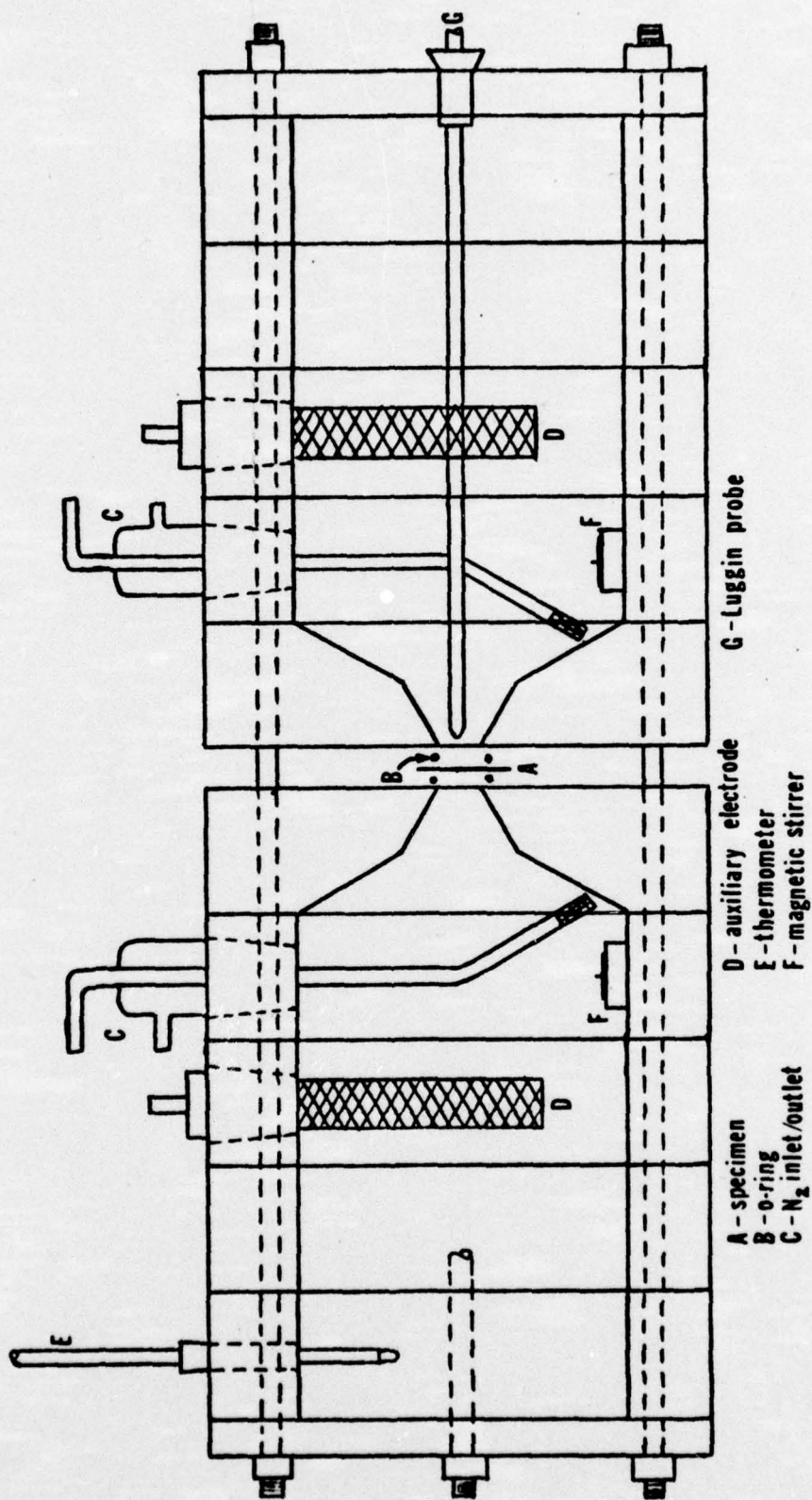


Figure 3: Hydrogen permeation cell used in this investigation. Container is constructed of Teflon with plexiglass ends.

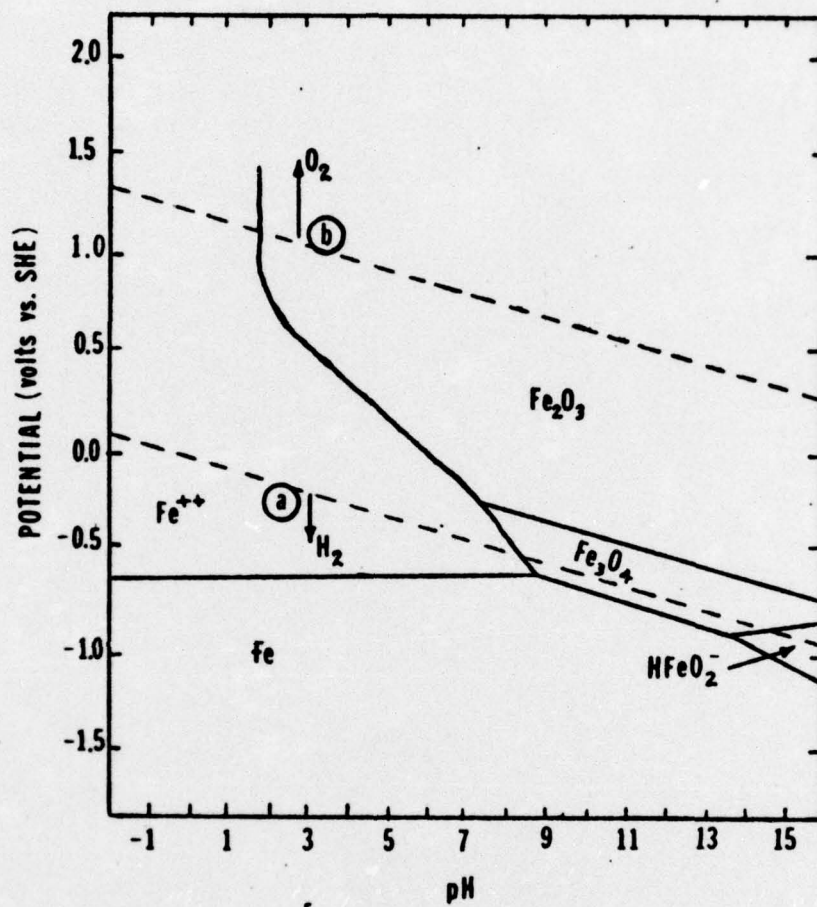


Figure 4: Potential - pH (Pourbaix) diagram for iron. (Reference 37.)

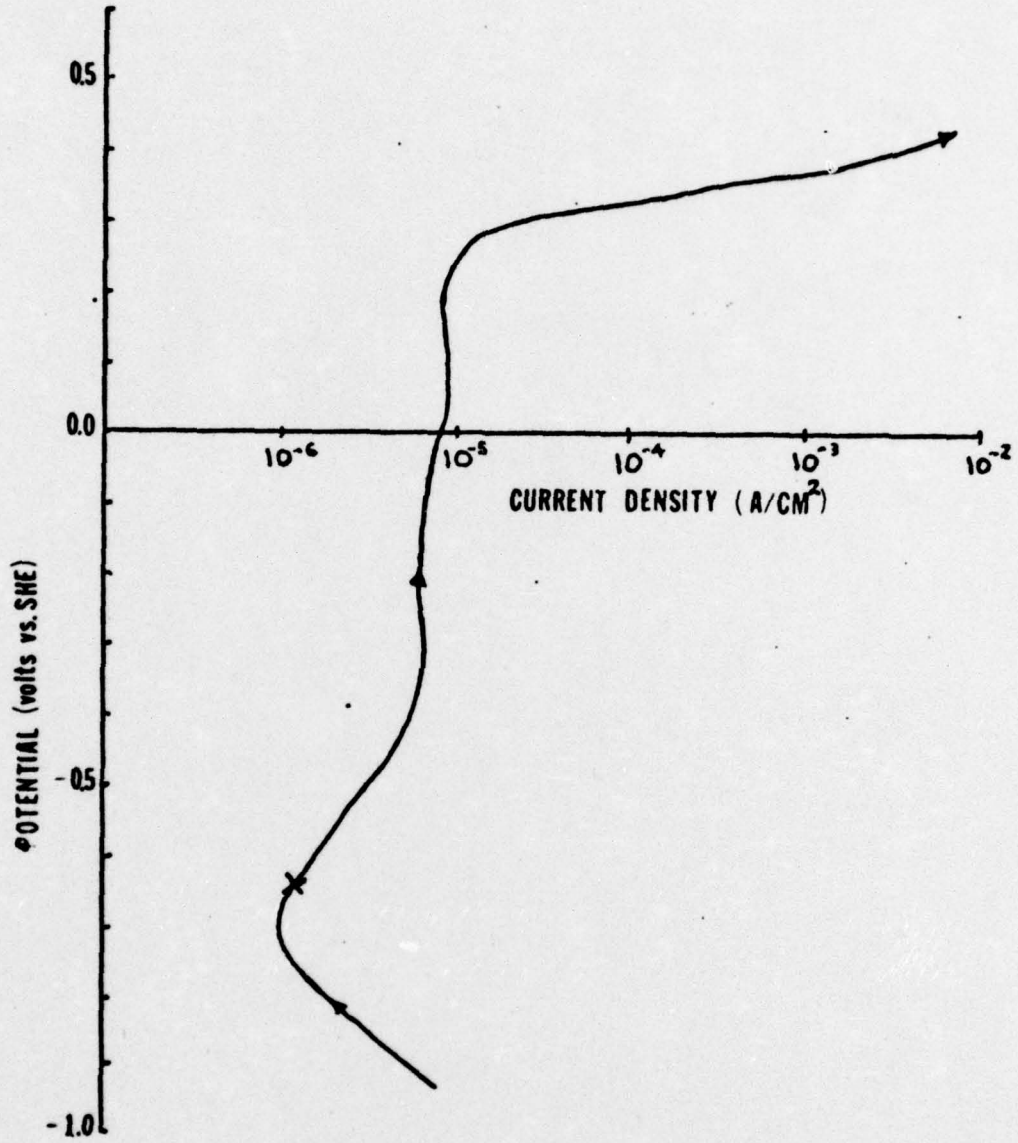


Figure 5: Polarization curve for Armco iron in 0.2N NaOH.

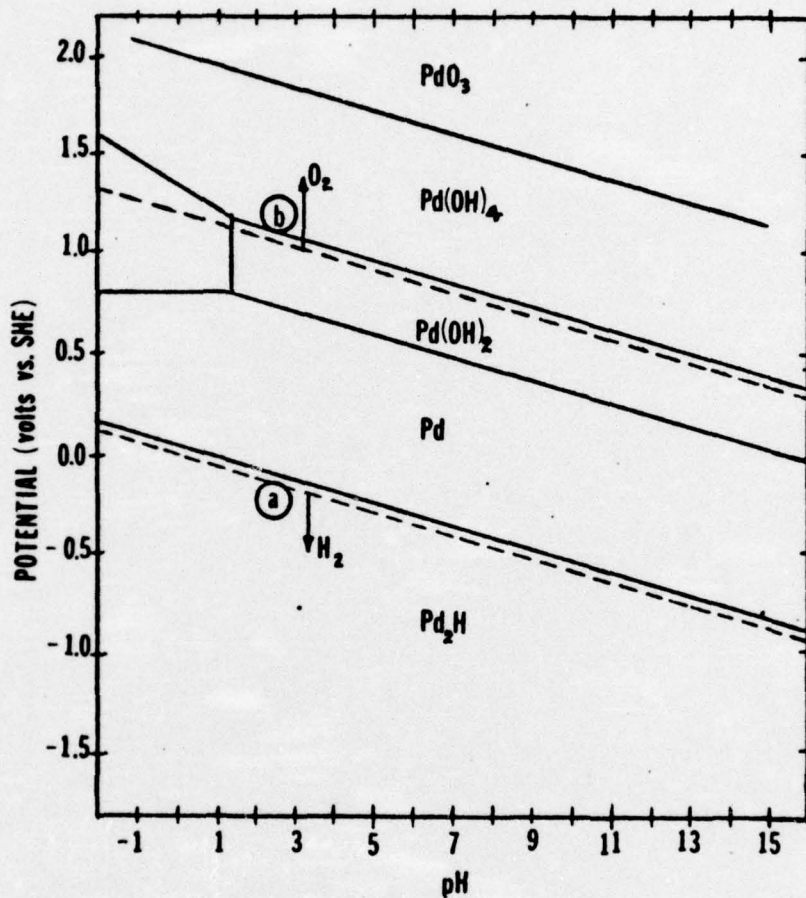


Figure 6: Potential - pH (Pourbaix) diagram for palladium. (Reference 37.)

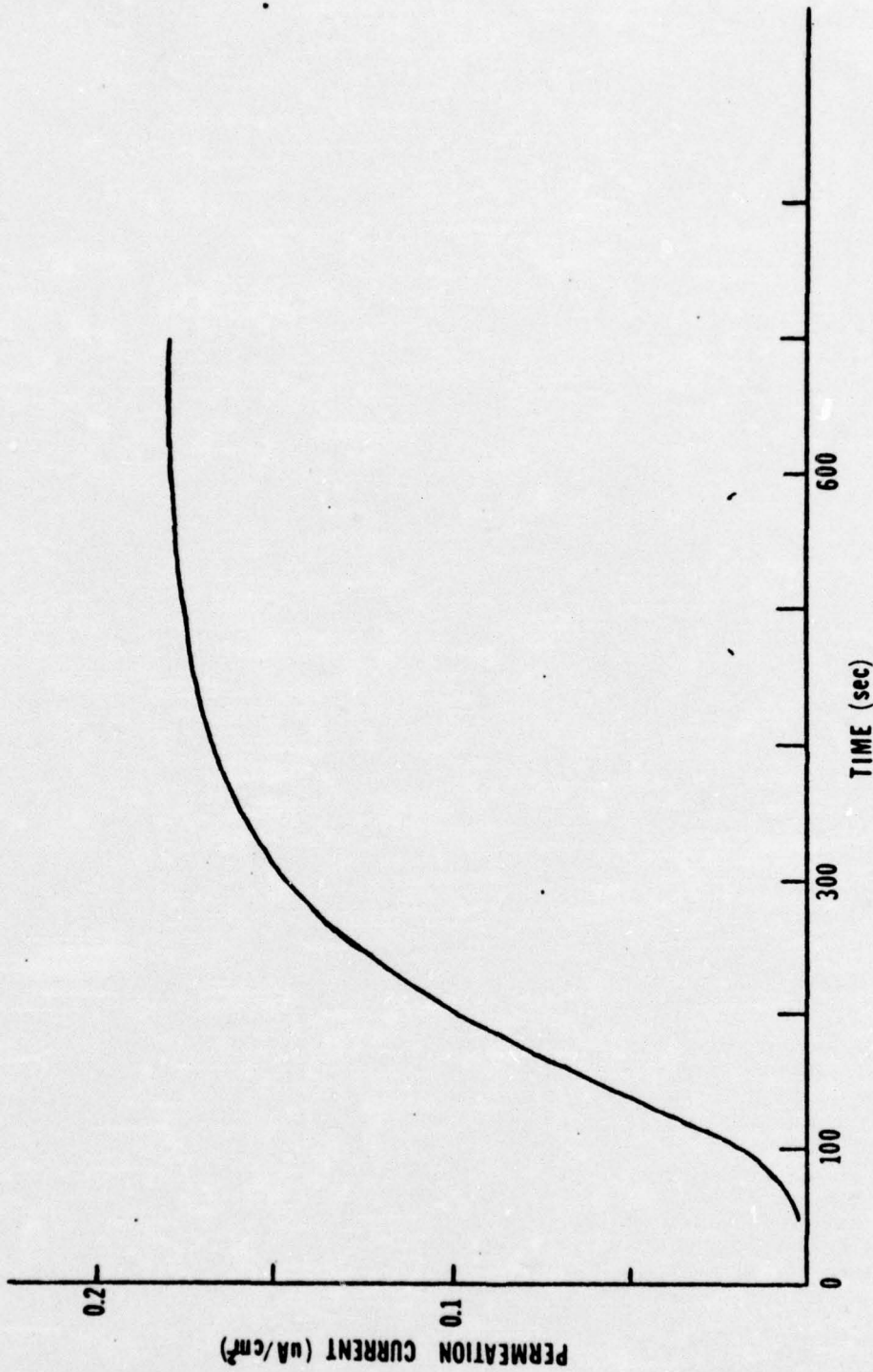


Figure 7: Typical hydrogen permeation transient previously reported for palladium-coated Armco iron. Charging current density = 1.75 mA/cm², thickness = 0.200 cm, temperature = 300°K. (Redrawn from A. Kumnick, Ph. D. dissertation, Reference 19.)

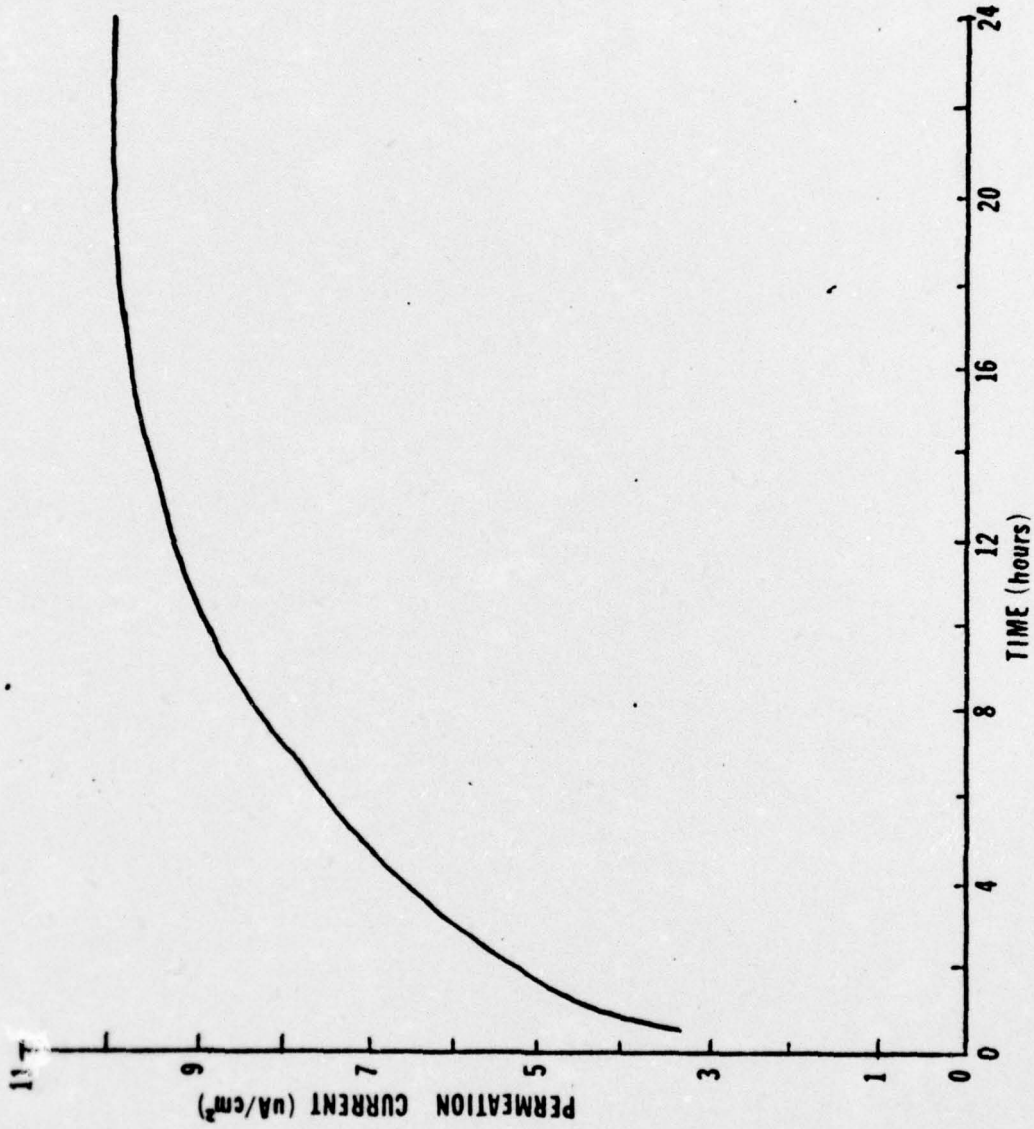


Figure 8: Typical hydrogen permeation transient for palladium-coated Armco iron obtained in this study. Charging current density = 5.21 ma/cm², thickness = 0.053 cm, temperature = 24 ± 3°C. Palladium applied by vapor deposition, approximately 1200 Angstroms thick.

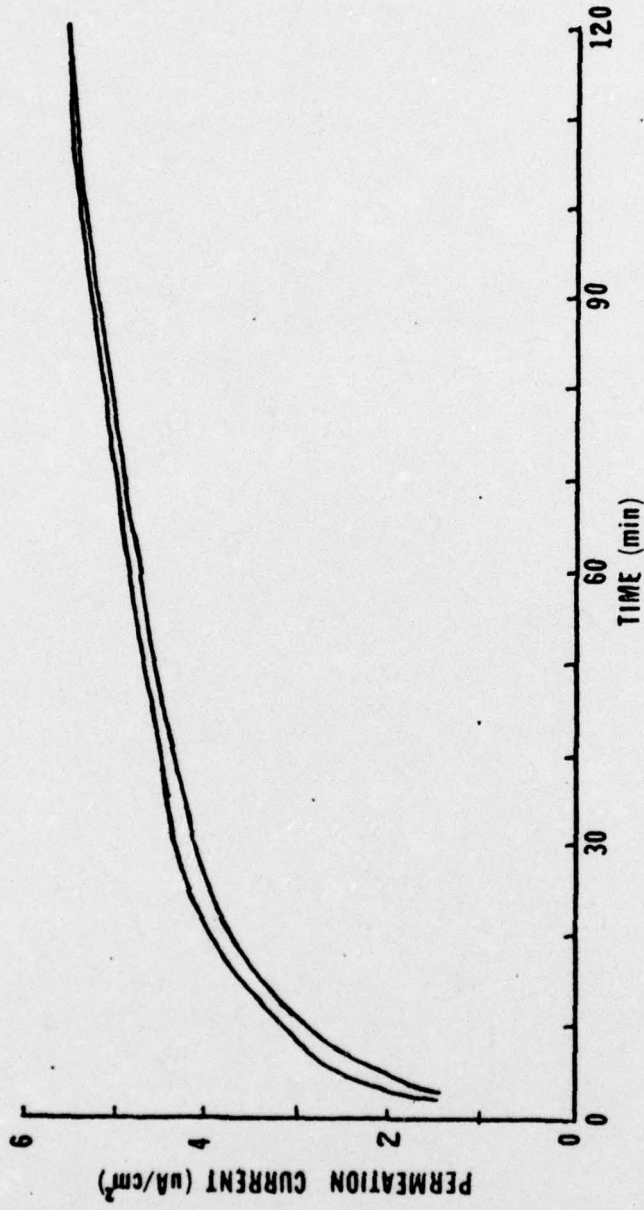


Figure 9A: Replicate hydrogen permeation transients for Armco iron with vapor deposited entry and exit surfaces.

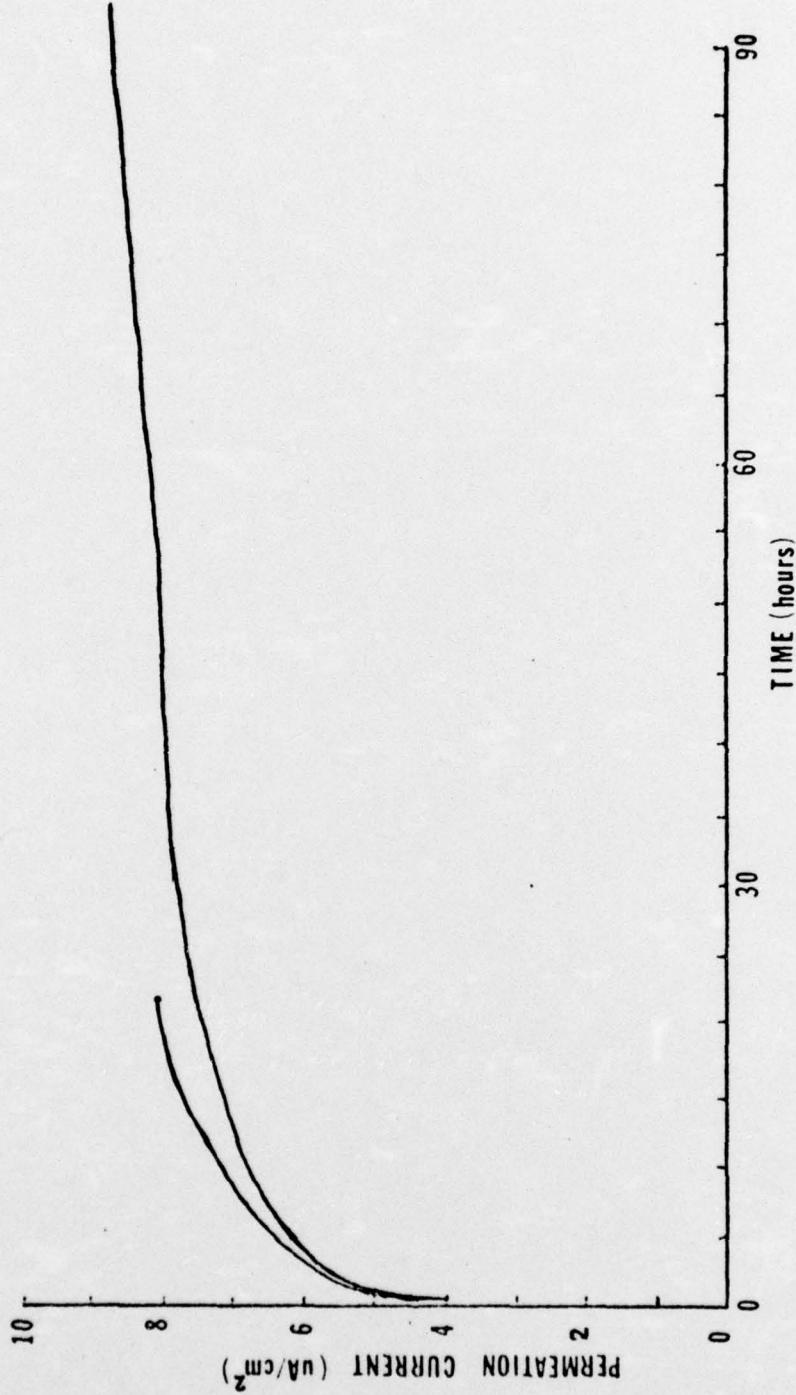


Figure 9B: Replicate hydrogen permeation transients for Armco iron with vapor deposited entry and exit surfaces.

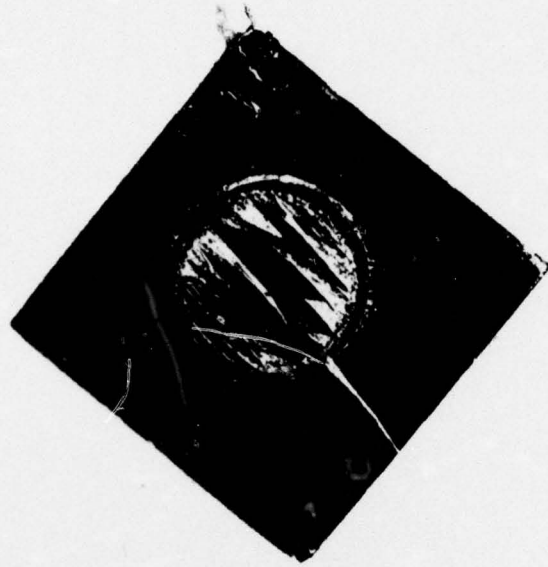


Figure 10: Debonded palladium coating after prolonged hydrogen charging.

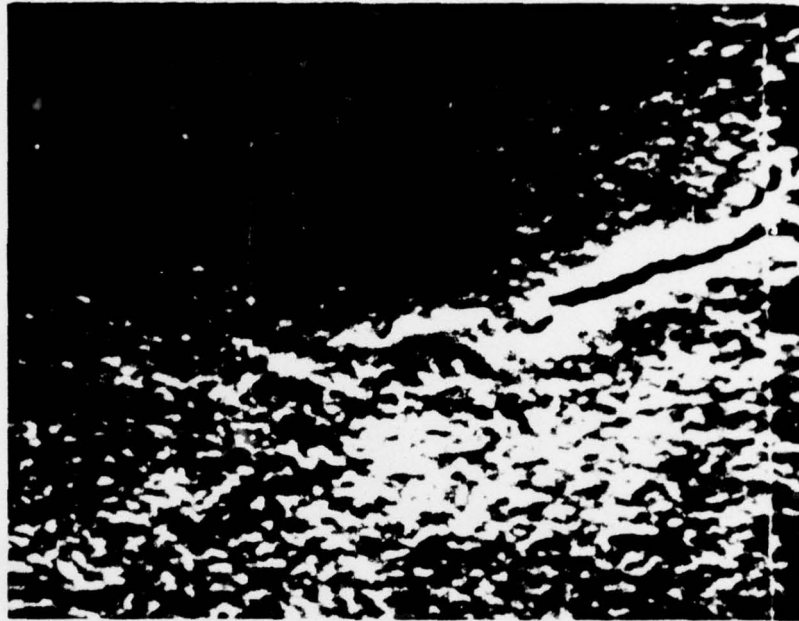


Figure 11: Blistering of electrodeposited palladium coating.

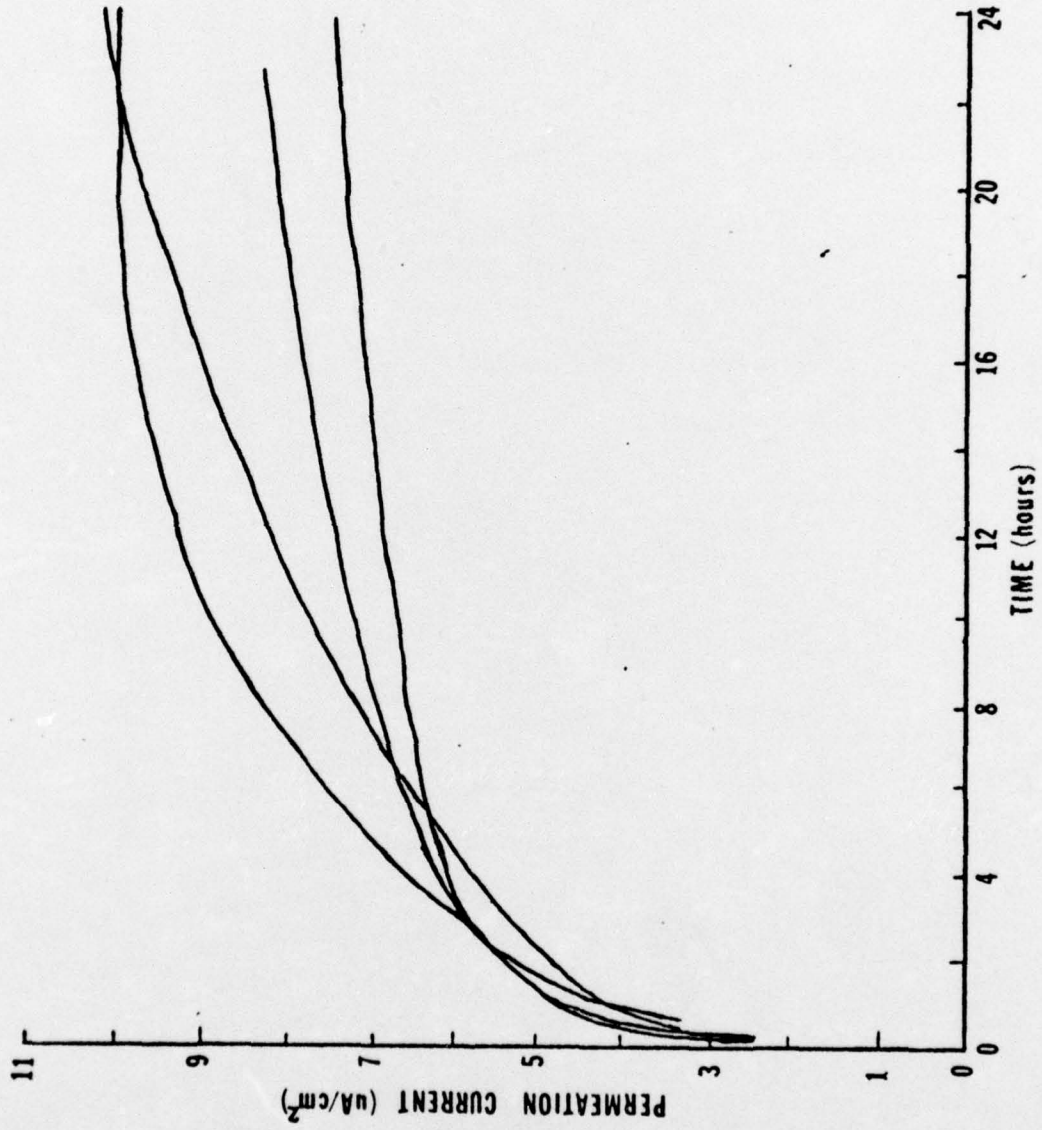


Figure 12: Hydrogen permeation transients for plasma-coated and vapor-deposited Armco iron. Plasma-coated transients have the higher long-term permeation currents.

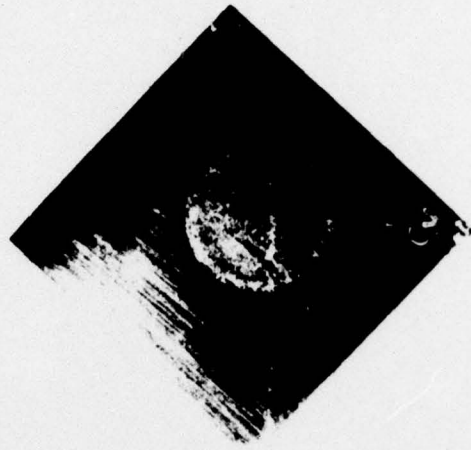


Figure 13: Tarnish film on surface of palladium coated sample.

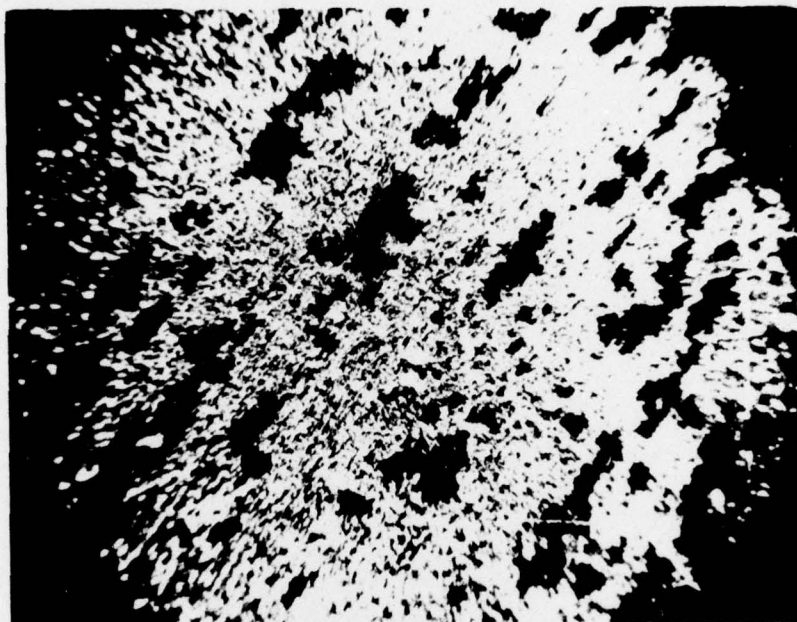


Figure 14: Micrograph of surface in Figure 13.

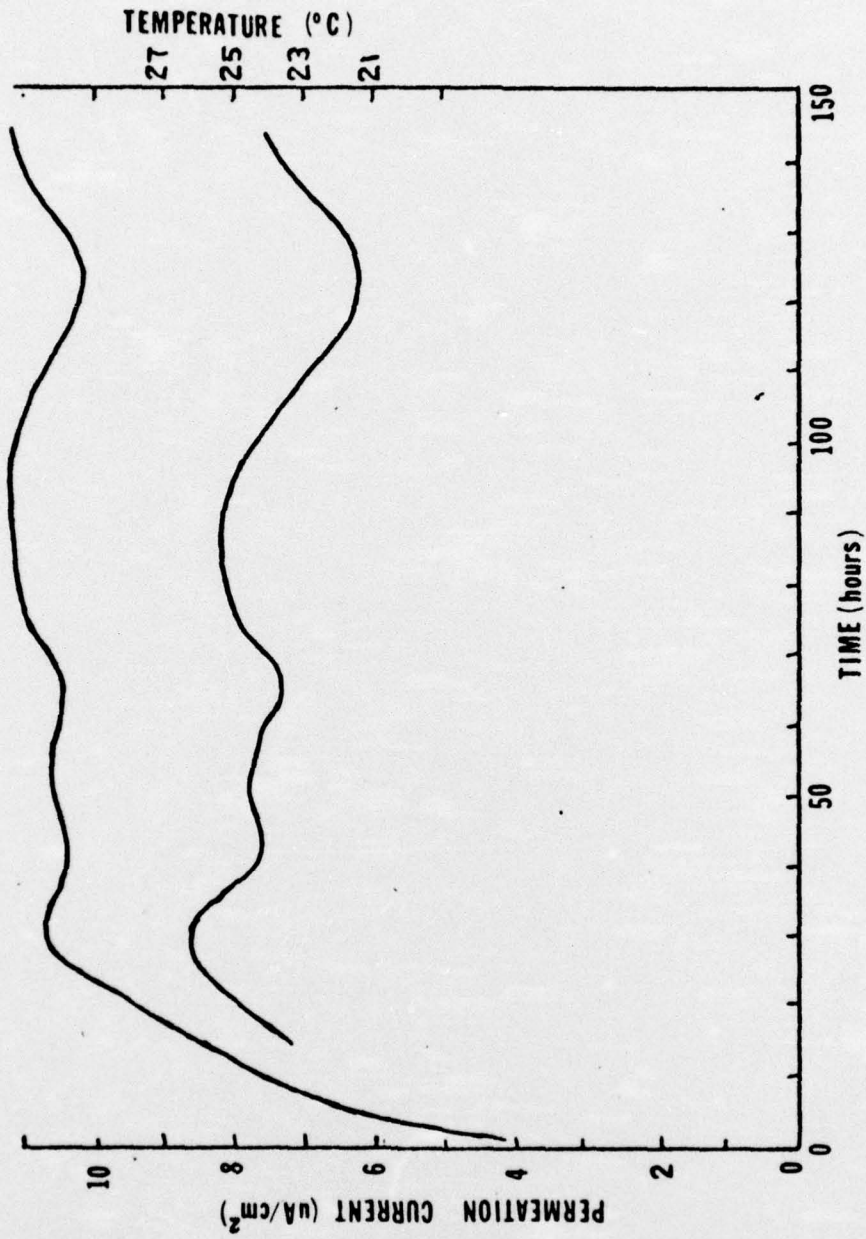


Figure 15: Effect of temperature on measured permeation current.

APPENDIX A: POTENTIOSTAT DESIGN FABRICATED FOR THIS STUDY

Potentiostat Specifications

Control Range: ± 1.00 Volts with respect to the reference electrode

Maximum Current Output: Approximately 1 Milliampere

Reference Electrode Current: Less than 1 Picoampere

Reference Voltage: ± 1.00 Volt Obtained from Regulated (± 15 VCD) Supply

Potential Drift: Less than 10 Millivolts

Supply Voltage: ± 15 VDC, Regulated .5% Line, .5% Load

Theory of Operation:

The circuit is based upon a voltage feedback system, using A2 as an inverting amplifier utilizing negative feedback. The non-inverting terminal is referred to ground while feedback resistor R_5 is placed in-between the inverting and output terminals. Resistor R_4 is placed in series with the signal source E_s and the inverting terminal.

It can be shown that the output signal E_o , will be

$$E_o = -A(E_s - bE_o) \quad \text{where}$$

A = Gain of the Amplifier (A_2), R_5/R_4

E_s = Input Signal

b = Fraction of the output signal fed back, and

E_o = Output Signal.

If $bE_o = E_s$, then the voltage between the auxiliary and working electrodes, E_o , and, therefore, the current, will be zero. Thus a difference between bE_o and E_s will cause a non-zero output which tends to bring bE_o and E_s back to equivalence.

Amplifier A1 is set up as a high impedance voltage follower for the input of the reference electrode. Utilizing the extremely high input impedance of A1 enables the life , the reference electrodes to be indefinite.

Switch S1 allows the polarity of the reference voltage to be varied. Potentiometers R1 and R2 allow the reference voltage to be accurately set.

Parts List:

<u>Part Number</u>	<u>Description</u>
A1	Analog Devices Ad 515 Operational Amplifier
A2	National Semiconductor LM 308 Operational Amplifier
R1	25K Trim Potentiometer
R2	1K 10 Turn Precision Potentiometer
R3(2)	1M, 10%, 1/4 Watt Resistor
R ₄ (2)	1.2M, 10%, 1/4 Watt Resistor
R ₅	22M, 10%, 1/4 Watt Resistor
C1	0.0082 uf, 1Kv Capacitor
S1	Spdt Switch

Miscellaneous: Regulated power supply, knobs, jacks, terminals, cabinet

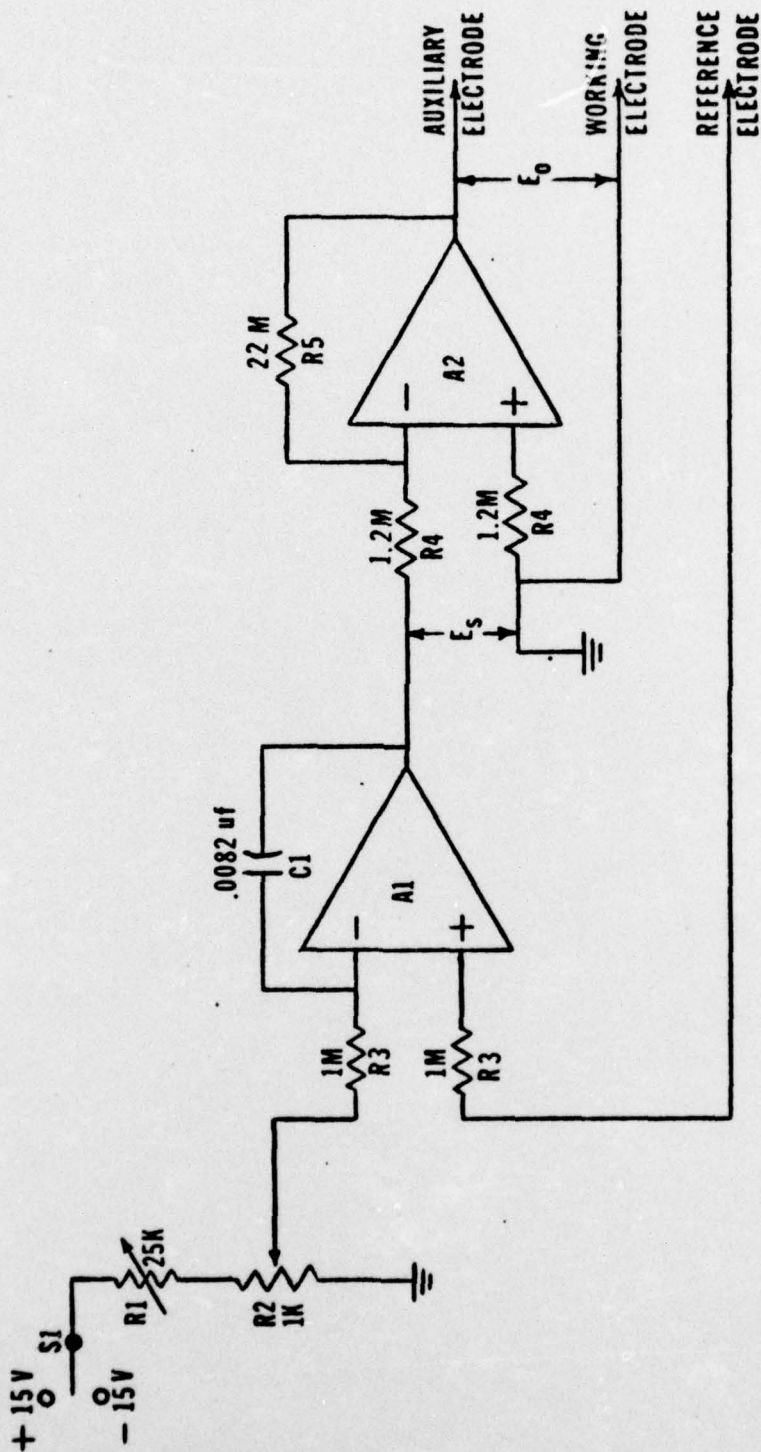


Figure A1: Schematic of potentiostat fabricated for this study.

APPENDIX B: REGULATED-CURRENT D. C. POWER SUPPLIES
FABRICATED FOR THIS STUDY

Parts List

<u>Part Number</u>	<u>Description</u>
1C1	RCA CA723C Integrated Circuit
R1	18 Ω , 10%, 1/4 Watt Resistor
R2	10K Ω , Trim Potentiometer
R3	33K Ω , 10%, 1/4 Watt Resistor
C1	100 pF, 1KV, Capacitor
D1	IN 457, Diode

Miscellaneous: 15 V DC Regulated Power Supply, Terminals, Ammeter,
Switches, Chassis

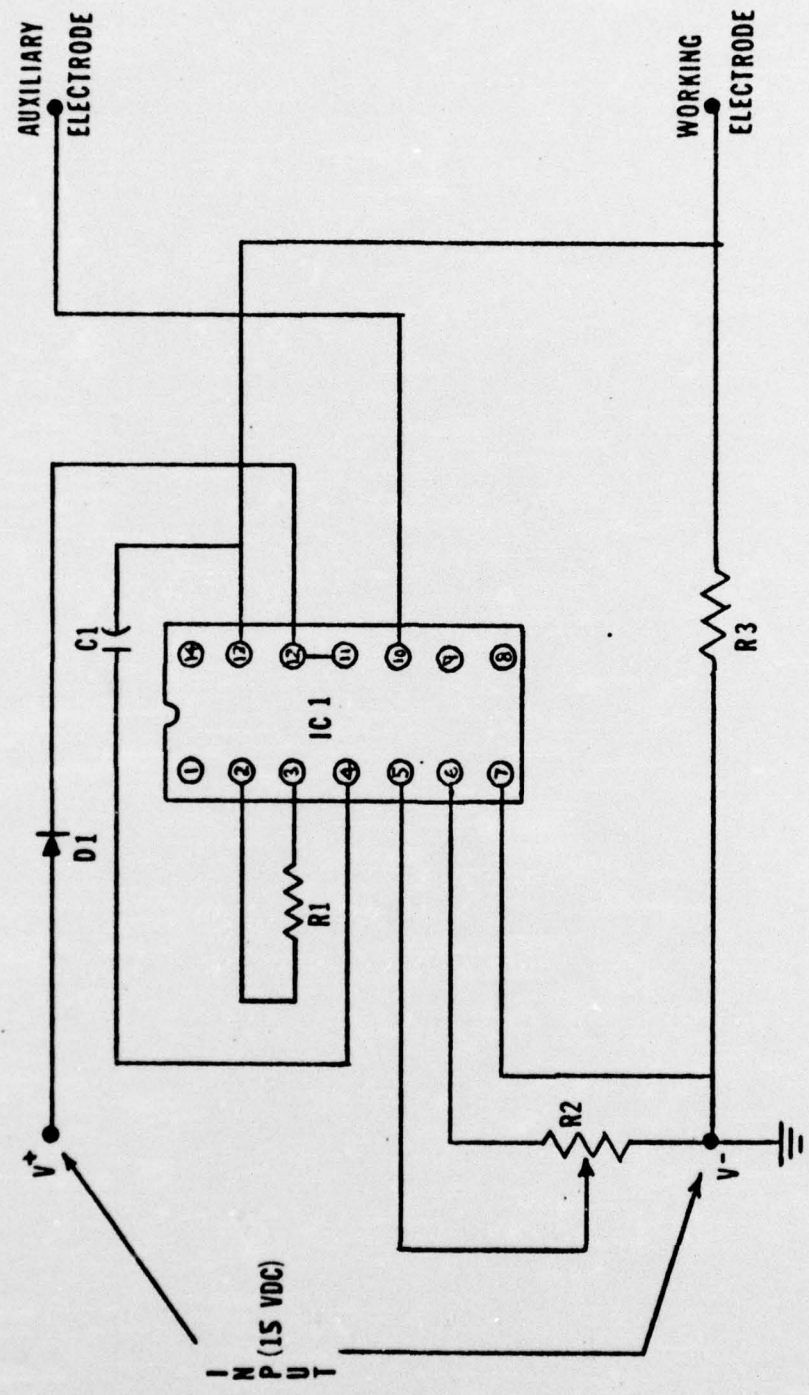


Figure B1: Schematic of regulated-current D. C. power supply fabricated for this study.

APPENDIX C. CALCULATIONS AS TO WHETHER PALLADIUM COATINGS
WILL BE RATE LIMITING FOR HYDROGEN TRANSPORT

The use of the palladium coatings on both the inlet and exit surfaces of the specimens has certain advantages which have been discussed previously in the report. It is necessary, however, to be certain that it is not the palladium which is limiting the diffusion, but rather the iron.

An order of magnitude calculation can be obtained to compare the potential flux across the Pd layer as compared to that across the iron. The steady state flux can be represented as follows:

$$J_{\infty} = D \frac{C_0}{L}$$

	Fe	Pd
D (cm ² /sec)	= 10 ⁻⁵	= 10 ⁻⁷
C ₀ (Arbitrary Units)	1	100
L (cm)	5 x 10 ⁻²	2 x 10 ⁻⁵

$$\frac{J_{\infty \text{ Pd}}}{J_{\infty \text{ Fe}}} = \frac{10^{-7} (100/2 \times 10^{-2})}{10^{-5} (1/5 \times 10^{-2})} = 2.5 \times 10^3 \quad (\text{Ref. 19})$$

Coupled with the fact that for identical samples, one with a palladium coated inlet surface and one without, the coated sample produces the higher flux, there is little doubt that it is the iron layer which is rate limiting and not the palladium. This calculation is identical in method to that used in A. Kumnick, Ph. D. Dissertation, Cornell University, 1972 (Reference 19).